Talanta 81 (2010) 591–596

Contents lists available at ScienceDirect

Talanta

journal homepage: www.elsevier.com/locate/talanta

A novel fluorescent vesicular sensor for saccharides based on boronic acid–diol interaction

Yujian Zhang, Zhenfeng He, Guowen Li*

State Key Laboratory of Supramolecular Structure and Materials, Jilin University, 2699 Qianjin Avenue, Changchun, Jilin Province 130012, China

ARTICLE INFO

Article history:
Received 28 September 2009
Received in revised form
22 December 2009
Accepted 22 December 2009
Available online 4 January 2010

Keywords:
Fluorescence vesicular sensor
Saccharide
Boronic acid
Amphiphiles

ABSTRACT

A novel amphiphile containing two functional groups of both naphthalene and boronic acid, 2-(hexadecyloxy)-naphthalene-6-boronic acid (HNBA), has been synthesized. Scanning electron microscopy (SEM) indicated the formation of bilayer vesicles in the ethanol/water solution ($\Phi = 0.6$). Differential scanning calorimetry (DSC) established the presence of crystal-to-liquid crystal transition at 63.36 °C. The vesicular fluorescence properties upon binding with carbohydrates have been studied in ethanol/water buffer at pH 7.4. Addition of saccharides to the vesicular solution, the fluorescent intensities of naphthalene in HNBA vesicles centered at 348 nm decreased dramatically with increasing concentration of saccharides. The change tendency of fluorescent intensities of the HNAB vesicles with concentration of saccharides followed in the order of fructose > galactose > maltose > glucose. The pH profiles of the fluorescence intensity were studied in the absence and in the presence of sugars. Also, the urine sample induced spectral changes of the HNBA vesicles were studied. These results suggest that the HNBA vesicles may be developed as a continuous monitoring and implantable fluorescence vesicular sensor, which might be applied in the practical field.

1. Introduction

The design and preparation of effective fluorescent chemosensors for biologically relevant analytes is of paramount interest in supramolecular chemistry [1]. Saccharides are nature's conveyors of energy and therefore essential for cell survival [2]. The breakdown of glucose transport has been correlated with certain diseases such as diabetes [3]. It is therefore unsurprising that receptors with the capacity to detect chosen saccharide selectively and signal this presence by altering their optical signature have attracted considerable interest in recent years [4–6]. To date, a wide variety of methods for saccharide analysis have been reported in the research literature, including electrochemistry [7], near infrared spectroscopy [8], optical rotation [9], colorimetric [10] and fluorescence detection [11]. The most commonly used technology for blood glucose determination is an enzyme-based method [11], which requires frequent collection of blood samples. However, this method is an inconvenience, which affects compliance by patients and is not a continuous monitoring. Recently, there is a great deal of interest in the development of continuous glucose monitoring systems, which would be able to provide patients with instantaneous glucose concentration [12,13]. Chemical sensors can offer the advantage of higher stability, continuous glucose monitoring, and relatively easy manufacturing. Especially, fluorescent sensors are preferred because they are well suited to meet the need for in vivo probes. Such a concept has already been put into test by companies such as sensors for medicine and science [14]. To develop a practical sensor based on continuous monitoring system, it would be ideal to use an implantable device that is in constant contact with the biological fluid to give a continuous reading of glucose concentration. Supramolecular aggregates may provide promising carriers for implantable and continuous monitoring sensors. Along this line, we are interested in the development of fluorescent sensors for saccharide in the vesicular systems [15].

The phospholipid bilayer vesicles are well-studied biomembrane mimics, which have wide biomedical applications for drug delivery, biological sensors and artificial blood [16]. Also, the artificial amphiphiles can form vesicles in dilute aqueous solution [17]. The vesicles might be used as artificial membrane models [18]. If some functional groups are introduced into an artificial amphiphilic molecule, such as fluorophore and recognizable group, the amphiphile could form vesicular receptor which might be used as an implantable carrier for a sensor.

Following the pioneering works of Yoon and Czarnik [19] and later Sandanayake and Shinkai [20], boronic acid derivatives have been used in the recognition and sensing of vicinal diols, carbohydrates, and catechols for the past two decades [21]. Boronic acids are known to bind with compound containing diol moieties through reversible ester formation [22]. Such bonding allows

* Corresponding author. Tel.: +86 431 85168485; fax: +86 431 85193421.
E-mail address: lgw@mail.jlu.edu.cn (G. Li).

0039-9140/$ – see front matter © 2010 Elsevier B.V. All rights reserved.
doi:10.1016/j.talanta.2009.12.041

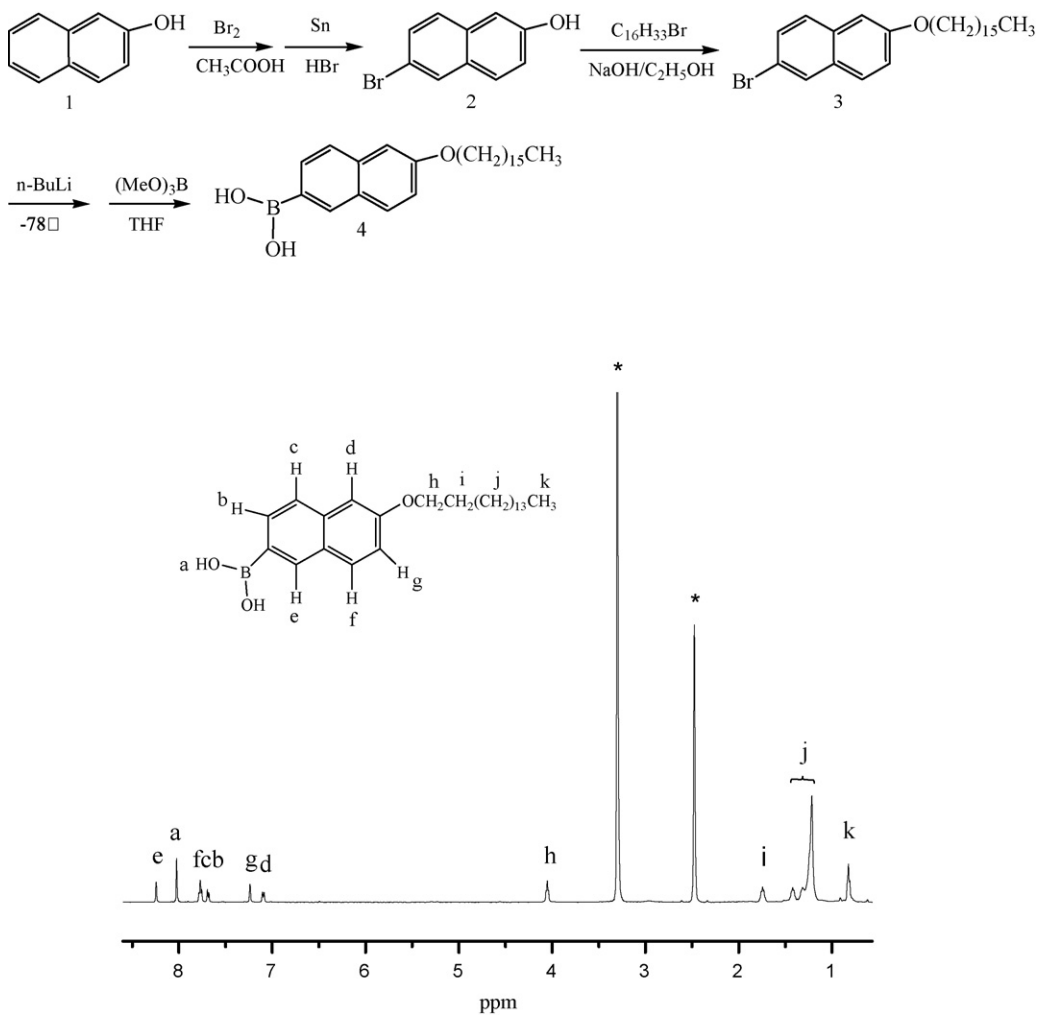

Scheme 1. Synthetic route and ^{1}H NMR spectrum of 2-(hexadecyloxy)-naphthalene-6-boronic acid (4, HNBA) amphiphile.

boronic acids to be used as the recognition moieties in a sensor for saccharides [4]. James et al. [23], Wang et al. [24] and Geddes et al. [25] have developed many novel sensors composed of small organic molecules based on interaction between boronic acids and saccharide. However, these systems reported could not be implantable.

Herein, we have developed a novel vesicular sensor composed of HNBA amphiphile, which contained both boronic acid and naphthalene "read-out" unit. The HNBA vesicles might be used as a continuous monitoring and implantable fluorescence vesicular sensor for the saccharides.

2. Experimental

2.1. Materials

2.1.1. Chemicals

All chemicals were of the highest purity commercially available: β-naphthol, 1-bromohexadecane and trimethyl borate were purchased from the Fluka (Japan). Bromine, tin, lithium, ethanol, THF, DMF, sodium hydroxide, sodium hydrogen carbonate, sodium sulfate anhydrous, glacial acetic acid, n-hexane, dichloromethane, methanol anhydrous and chloroform were purchased from Shanghai Biochemical Company, Beijing Chemical Company and Tianjing Tiantai Chemical Company, respectively. Reagents and solvents were used without further purification except as indicated below. Water is double distilled.

2.1.2. Synthesis

Compound 4, 2-(hexadecyloxy)-naphthalene-6-boronic acid (HNBA), was synthesized by the sequence outlined in Scheme 1.

2.1.3. 2-Hydroxyl-6-bromonaphthalene (2)

A mixture of β-naphthol (1.44 g, 10 mmol) and glacial acetic acid (4 ml) was added into 25 ml flask. Then bromine (3.2 g, 20 mmol) in glacial acetic acid (1 ml) was added dropwise in 15–30 min and the water (1 ml) was added. Reaction mixture stirred and refluxed for 15 min. After cooling down to 100 °C, tin (1.5 g, 12.7 mmol) was added into the solution and refluxed for 3 h. After cooling to 50 °C, the reaction solution was filtered and poured into ice/water solution (30 ml). The residue was filtered and washed with cold water to give pink crude product, which was recrystallized from chloroform/hexane (1:4) to give white solid 2 (1.52 g, yield: 68%). mp: 123–125 °C. ^{1}H NMR (500 MHz, $CDCl_3$) 7.92 (s, 1H, $-C_{10}H_6-$), 7.67 (d, 1H, $-C_{10}H_6-$), 7.56 (d, 1H, $-C_{10}H_6-$), 7.50 (d, 1H, $-C_{10}H_6-$), 7.11–7.12 (m, 2H, $-C_{10}H_6-$), 4.91 (s, 1H, –OH).

2.1.4. 2-Hexadecyloxy-6-bromonaphthalene (3)

2-Hydroxyl-6-bromonaphthalene (1.56 g, 7 mmol), 1-bromohexadecane (6.41 g, 21 mmol) and sodium hydroxide (about 0.3 g, about 7 mmol) were added into 50 ml of dry ethanol in 100 ml flask. The reaction mixture was stirred and refluxed for 12 h, and cooled in a refrigeratory for 6 h and 1-bromohexadecane was filtered. The crude residue was washed with water and ethanol

thrice respectively, dried in a desiccator to give a white solid of 3 (2.75 g, yield: 88%), mp: 55–57 °C. ^{1}H NMR (500 MHz, $CDCl_3$) δ: 7.91 (s, 1H, $-C_{10}H_6-$), 7.64 (d, 1H, $-C_{10}H_6-$), 7.59 (d, 1H, $-C_{10}H_6-$), 7.49 (d, 1H, $-C_{10}H_6-$), 7.17 (d, 1H, $-C_{10}H_6-$), 7.08 (s, 1H, $-C_{10}H_6-$), 4.06 (t, 2H, $-OCH_2-$), 1.84 (m, 2H, $-OCH_2CH_2-$), 1.25–1.49 (m, 26H, $-CH_2(CH_2)_{12}-$), 0.88 (t, 3H, $-CH_3-$).

2.1.5. 2-(Hexadecyloxy)-naphthalene-6-boronic acid (HNBA)

2-Hexadecyloxy-6-bromonaphthalene (1.83 g, 4 mmol) was added into 20 ml of dry THF in flask under N_2, stirred and cooled to −78 °C. Then a solution of n-BuLi in hexane (1 M, 5.6 ml, 5.6 mmol) was added dropwise into the reaction flask, stirred for 1 h and then $(MeO)_3B$ (1.55 ml, 13.6 mmol) was added. The reaction solution was stirred continuously for 1 h under −78 °C, and stirred overnight at room temperature. The solution was evaporated, and the residue was dissolved in 150 ml of dichloromethane, washed with 50 ml 0.1 M HCl and then with 5% $NaHCO_3$ to adjust the pH to 7, dried over $NaSO_4$, filtered. The filtrate was evaporated. The crude residue was purified by chromatography on silica gel (CH_2Cl_2:MeOH = 50:1, Rf = 0.43) to give white solid (1 g, yield 60%) of 4. mp: 77–79 °C. ^{1}H NMR (500 MHz, DMSO) δ: 8.27 (s, 1H, $-C_{10}H_6-$), 8.05 (s, 2H, $B(OH)_2$), 7.77–7.82 (m, 2H, $-C_{10}H_6-$), 7.72 (d, 1H, $-C_{10}H_6-$), 7.23 (s, 1H, $-C_{10}H_6-$), 7.12 (d, 1H, $-C_{10}H_6-$), 4.07 (t, 2H, $-OCH_2-$), 1.77 (m, 2H, $-OCH_2CH_2$), 1.23–1.45 (m, 26H, $-CH_2(CH_2)_{12}-$), 0.84 (t, 3H, $-CH_3$). Anal. Calcd. for $C_{26}H_{41}O_3B$: C, 75.76; H, 9.96. Found: C, 75.78; H, 9.98. Also, the ^{1}NMR spectrum of the HNBA compound is shown in Scheme 1.

2.2. Preparation of HNBA vesicles [17]

The HNBA amphiphile was dissolved in spectroscopic grade $CHCl_3$. Solvent was removed under a N_2 flow, followed by evaporation at high vacuum for 0.5 h. The ethanol/water (Φ = 0.6) solution was added into the resulting cast film in beaker. The concentration of HNBA amphiphile was fixed at 1×10^{-5} mol/l. The solution was sonicated by a bath-type sonicator (40 kHz 100 W KQ-100, Shanghai of China) for 4 h at about 60 °C. The vesicular solution was then cooled with ice-water bath for half an hour and then warmed to room temperature gradually. The sample dropped on silica plate, dried under room temperature for SEM determination.

2.3. Measurement

All ^{1}H NMR spectra were measured on a Brucker Avance 500 MHz spectrometer (Brucker Instruments, Germany) using a TMS proton signal as the internal standard. Melting points were determined with a Mel-Temp XT-40 micro melting point apparatus (JINGHE Analytical Instruments Co., Ltd. Instruments, Shanghai of China) and uncorrected. Scanning electron microscopy (SEM) images were collected on a JSM-6700F field emission scanning electron microscope (JEOL Instruments, Japan). Dynamic light scattering (DLS) were obtained using a Zetasizer Nano-ZS instrument (Malvern Instruments, UK, λ = 532 nm). The phase transition from crystal to liquid crystal (T_c) determined by differential scanning calorimetry (ca. 3 wt.%, DSC 204, NETZSCH Instruments, Germany). Steady-state fluorescence spectra were recorded on RF-5301PC spectrophotometer (SHIMADZU Instruments, Japan). Elemental analyses were carried out by Flash EA 1112 (Thermo Electron SPA Instruments, Italy) instrument at the Analysis and Determination Center of Jilin University.

3. Results and discussion

The stable HNBA vesicular morphologies were determined by scanning electron microscopy (SEM). The typical SEM image of HNBA amphiphile (1×10^{-5} M) is shown in Fig. 1. The diameters of vesicles were estimated about 450–1100 nm from Fig. 1. The sizes of the HNBA vesicles in ethanol/water solution were determined by DLS as shown in Fig. 2. The size distribution of HNBA vesicles is 737 (±1) nm which is consistent with the result of SEM image. The phase transition from crystal to liquid crystal (T_c) determined by means of differential scanning calorimetry is located at 63.36 °C (Fig. 3). These results supported that the HNBA amphiphile formed vesicles in ethanol/water solution [26].

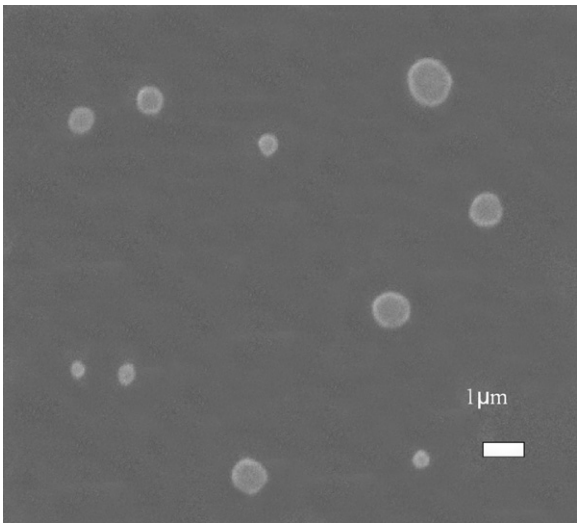

Fig. 1. SEM images of the HNBA vesicles in ethanol/water solution (1×10^{-5} M).

To understand the structural features associated with the fluorescence intensity changes, the pH profiles of the fluorescence intensity was studied in the absence and in the presence of fructose and glucose at a fixed concentration of 50 mmol (Figs. 4–6 respectively). Fig. 4 shows that a strong fluorescence peak at 348 nm decreased very slowly when pH increased from 3 to 7.4, and decreased quickly when pH increased from 7.4 to 10 in the absence of a sugar. The fluorescence intensity at 348 disappeared and 435 nm appeared at pH 10, which increased very quickly when pH increased from 10 to 11. The pH-induced spectral changes at 348 nm, in the presence of fructose and glucose (50 mmol), are similar to those in the absence of a sugar as shown in Fig. 5. The pH-induced spectral changes at 435 nm are shown in Fig. 6.

In order to help to understand the assignment of each fluorescent peak, Scheme 2 could be used to show the various ionization states of HNBA vesicles in the various pH solutions. At low pH ≤ 7.4,

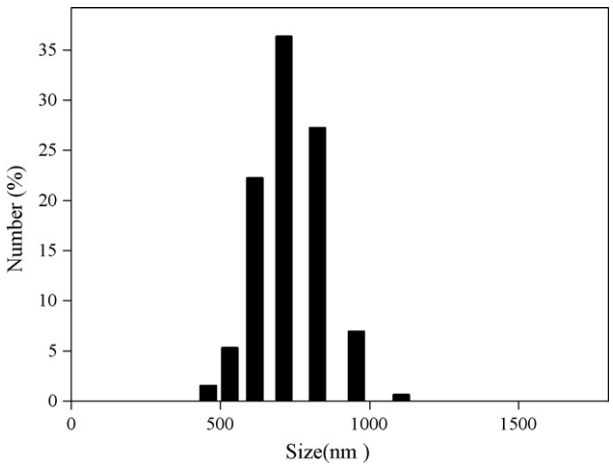

Fig. 2. Particle size distribution of HNBA vesicles in ethanol/water solution (1×10^{-5} M).

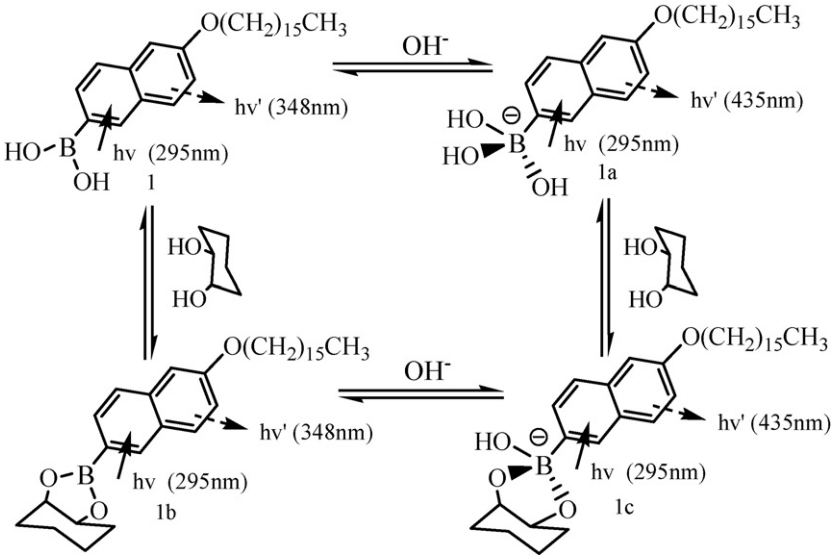

Scheme 2. Fluorescence properties of HNBA vesicles in different ionization states, in the absence and in the presence of a sugar in ethanol/water buffer.

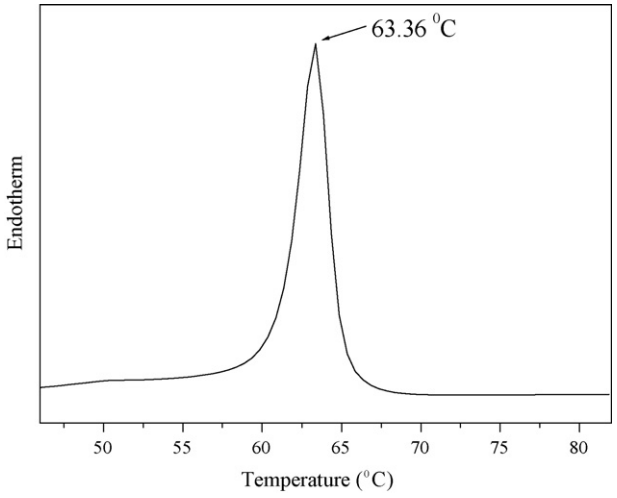

Fig. 3. DSC thermogram of the HNBA vesicular solution (3%).

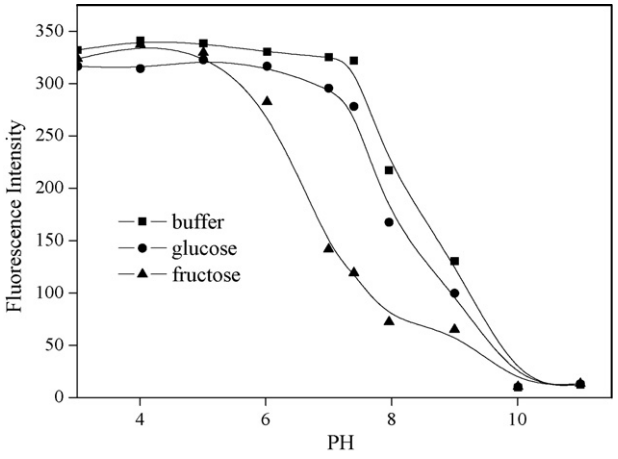

Fig. 5. pH-dependent fluorescence intensity changes of HNBA (1×10^{-5} mol/l) at 348 nm in the absence and in the presence of sugar (50 mmol) in ethanol/water ($\Phi = 0.6$) buffer, $\lambda_{ex} = 295$ nm.

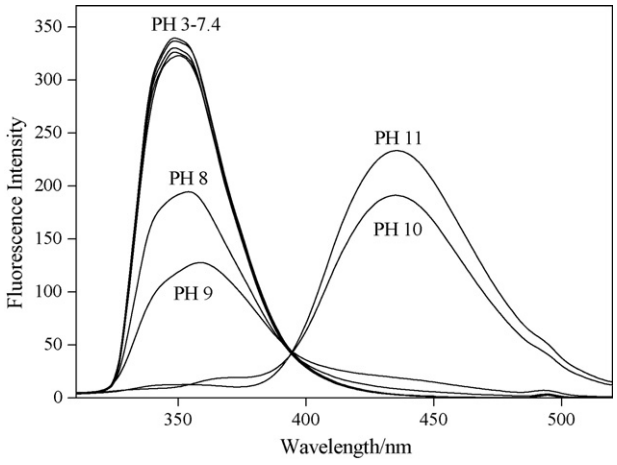

Fig. 4. Fluorescence spectral changes of HNBA (1×10^{-5} mol/l) in the absence of sugar at different pH in ethanol/water ($\Phi = 0.6$) buffer, $\lambda_{ex} = 295$ nm.

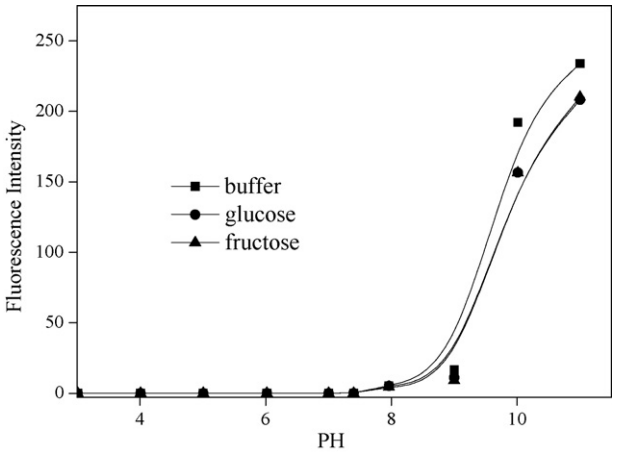

Fig. 6. pH-dependent fluorescence intensity changes of HNBA (1×10^{-5} mol/l) at 435 nm in the absence and in the presence of sugar (50 mmol) in ethanol/water buffer ($\Phi = 0.6$), $\lambda_{ex} = 295$ nm.

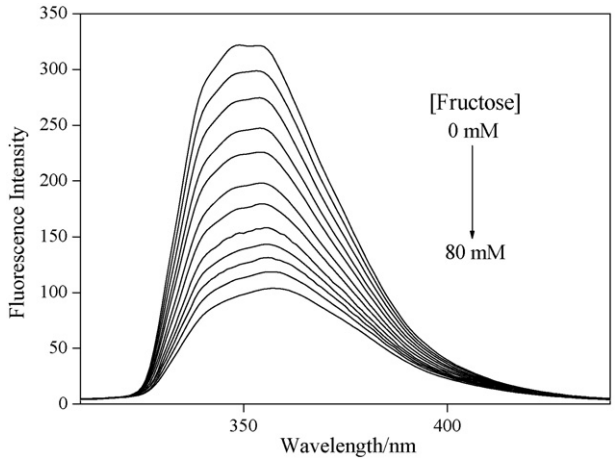

Fig. 7. Fluorescence spectral changes of HNBA vesicular solution (1×10^{-5} M) at different concentrations of fructose (0–80 mM) in ethanol/water ($\Phi = 0.6$) buffer at pH 7.4; $\lambda_{ex} = 295$ nm, $\lambda_{em} = 348$ nm.

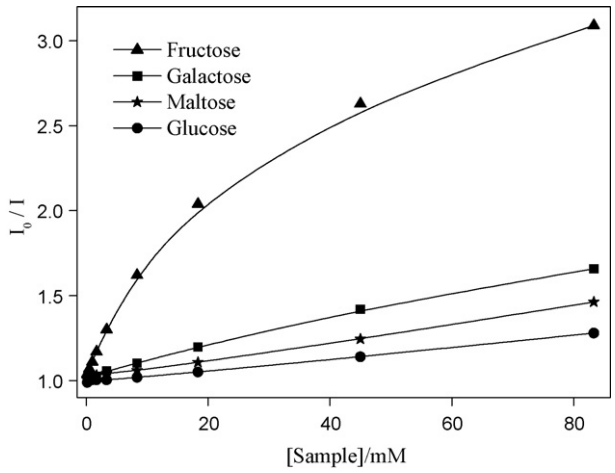

Fig. 8. Fluorescence intensity changes of HNBA vesicular solution (1×10^{-5} M) as a function of sugar concentration in ethanol/water ($\Phi = 0.6$) buffer at pH 7.4 in the absence, I_0, and in the presence, I, of sugars, $\lambda_{ex} = 295$ nm, $\lambda_{em} = 348$ nm.

the strongest fluorescent peak is the one at 348 nm in the absence and in the presence of a sugar. This corresponds to the naphthalene with a boronic acid in a neutral trigonal state such as 1 and 1b in Scheme 2. As the pH increases, the peak intensity at 348 nm decreases and gradually disappeared, and the one at 435 nm concomitantly appeared and increased. This change correlates with a transition of a neutral trigonal boronic acid (1 or 1b) to its corresponding anionic tetrahedral species (1a or 1c). This change is consistent with the result reported by Gao et al. [27].

The fructose induced fluorescence changes of the HNBA vesicles were studied. In general, the selective vesicular solution in ethanol/water ($\Phi = 0.6$) buffer was titrated by means of adjustable quantitative liquid shifter with aqueous solution of sugars at various concentrations, and then the fluorescence intensity was recorded. The typical fluorescence spectra are shown in Fig. 7 when aqueous fructose solution was added dropwise into the HNBA vesicular solution at pH 7.4. It is clear that the fluorescent intensities of naphthalene in HNBA vesicles centered at 348 nm decreases dramatically with increasing concentration of fructose from 0 to 8×10^{-2} M, which suggest the boronic acid formed boronate ester with fructose [20,28]. Also, this change is consistent with the result reported by Gao et al. [27].

To examine the general applicability of this fluorescent vesicular sensor, we have also studied the effect of three other carbohydrates on its fluorescence intensity. These carbohydrates include galactose, maltose and glucose. The corresponding titration curves obtained by plotting I_0 divided I, where I_0 and I are the fluorescence intensity values at 348 nm in the absence and in the presence of sugars, respectively, versus sugar concentration are shown in Fig. 8. A 3.09-, 1.65-, 1.46-, 1.28-fold decrease in fluorescence intensity with 80 mM fructose, galactose, maltose and glucose are respectively observed in HNBA vesicles. From Fig. 8, it is clear that all four carbohydrates tested caused significant fluorescence intensity decrease at physiological pH with varying magnitude. The change tendency for fluorescent intensities of the HNBA vesicles with the saccharides is similar to the other systems to favor the binding with fructose over galactose, maltose and glucose. To examine the binding more quantitatively, the association constants K_a between HNBA vesicular sensor and the four carbohydrates were determined, assuming the formation of a 1:1 complex [29]. The affinity trend of the vesicular sensor followed in the order of fructose > galactose > maltose > glucose (see Table 1). Indeed, these binding constants are similar to those observed with boronic acid in other system [27].

Table 1
Association constants (K_a) and maximal fluorescence intensity changes ($\Delta I/I_0$) of HNBA sensor at 348 nm with different sugars.

Sugar	K_a (M^{-1})	$\Delta I/I_0$ (sugar concentration (M))
Fructose	237 ± 21	−0.60 (0.05)
Galactose	61 ± 7	−0.29 (0.05)
Maltose	44 ± 5	−0.19 (0.05)
Glucose	27 ± 2	−0.13 (0.05)

In order to explore its potential application, urine samples of diabetic patients induced spectral changes of the HNBA vesicles can be seen in Fig. 9. It is clear that the fluorescent intensities of naphthalene in HNBA vesicles centered at 348 nm decreased dramatically with increasing concentration of the urine glucose from 0 to 1.75 mM. A 1.96-fold decrease in fluorescence intensity with 1.75 mM urine glucose is observed from the inset of Fig. 9. Interestingly, the vesicles show a ≈49% intensity change in the presence of as little as 1.75 mM urine glucose, noting that the normal urine glucose levels can change from ≈0.1 nM to 0.9 mM for a person [30]. This result implies that the HNBA vesicular sensor might be applied to a practical field.

Boronic acids provide us with the potential recognition group by taking advantage of the covalent bond formation between recep-

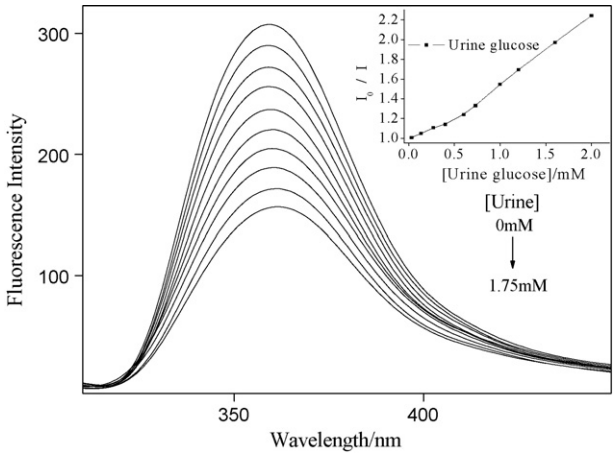

Fig. 9. Fluorescence spectral changes of HNBA vesicular solution (1×10^{-5} M) at different concentrations of urine sugar (0–1.75 mM) in ethanol/water ($\Phi = 0.6$) buffer at pH 7.4; inset: the 348 nm emission intensity ratio for in absence, I_0, and in the presence of urine sugar, $\lambda_{ex} = 295$ nm.

tors and saccharides. The vesicle provides us with a carrier which might be implantable. Therefore the fluorescence vesicular sensor may be developed as a practical one based on a continuous monitoring and implantable carrier, which might be applied in the practical field.

4. Conclusion

We have developed a novel fluorescence vesicular sensor. Fluorescence intensity changes of the vesicular solution with different saccharides were carried out in ethanol/water buffer at pH 7.4. The change tendency of fluorescent intensities of the HNBA vesicles with concentration of saccharides is similar to the other relative systems to favor the binding with fructose over other sugars. The order of selectivity of the vesicular receptor is fructose > galactose > maltose > glucose. Also, the urine glucose induced spectral changes of the HNBA vesicles were studied. These results suggest that the HNBA vesicles might be developed as a continuous monitoring and implantable carrier for a sensor, which might be applied in the practical field.

Acknowledgement

This work was supported by the National Science Foundation of China (Nos. 20874037, 20674025).

References

[1] P.A. Gale, Coord. Chem. Rev. 240 (2003) 17–55.
[2] R.N. Robertson, The Lively Membranes, Cambridge University Press, New York, 1983.
[3] H. Yasuda, T. Kurokawa, Y. Fuji, A. Yamashita, S. Ishibashi, Biochim. Biophys. Acta 1021 (1990) 114–118.
[4] T.D. James, S. Shinkai, Top. Curr. Chem. 218 (2002) 159–200.
[5] W. Ni, H. Fang, G. Springsteen, B. Wang, J. Org. Chem. 69 (2004) 1999–2007.
[6] M. Granda-Valdes, R. Badia, G. Pina-Luis, M.E. Diaz-Garcia, Quim. Anal. 19 (2000) 38–53.
[7] D.J. Claremont, I.E. Sambrook, C. Penton, J.C. Pickup, Diabetologa 29 (1986) 817–821.
[8] M.R. Robinson, R.P. Eaton, D.M. Haaland, G.W. Koepp, E.V. Thomas, B.R. Stallard, P.L. Robinson, Clin. Chem. 38 (1992) 1618–1622.
[9] B. Rabinovitch, W.F. March, R.L. Adams, Diabetes Care 5 (1982) 254–258.
[10] G.M. Schier, R.G. Moses, I.E.T. Gan, S.C. Blair, Diabetes Res. Clin. Pract. 4 (1988) 177–181.
[11] S. D'Auria, N. Dicesare, Z. Gryczynski, I. Gryczynski, M. Rossi, J.R. Lakowicz, Biochem. Biophys. Res. Commun. 274 (2000) 727–731.
[12] M. Gerritsen, J.A. Jansen, J.A. Lutterman, Neth. J. Med. 54 (1999) 167–179.
[13] P. Atanasov, S. Yang, C. Salehi, A.L. Ghindilis, E. Wilking, D. Schade, Biosens. Bioelectron. 12 (1997) 669–680.
[14] G.Y. Daniloff, Diabetes Technol. Ther. 1 (1999) 261–266.
[15] Q. Wang, G. Li, W. Xiao, H. Qi, G. Li, Sens. Acuators B 119 (2006) 695–700.
[16] S. Sofou, J.L. Thomas, Biosens. Bioelectron. 18 (2003) 445–455.
[17] T. Kunitake, Y. Okahata, J. Am. Chem. Soc. 99 (1977) 3860–3861.
[18] J.H. Fendler, Membrane Mimetic Chemistry, John Wiley & Sons, 1982, 113 pp.
[19] J. Yoon, A.W. Czarnik, J. Am. Chem. Soc. 114 (1992) 5874–5875.
[20] K.R.A.S. Sandanayake, S. Shinkai, J. Chem. Soc., Chem. Commun. (1994) 1083–1084.
[21] A. Robertson, S. Shinkai, Coord. Chem. Rev. 205 (2000) 157–199.
[22] J.P. Lorand, J.O. Edwards, J. Org. Chem. 24 (1959) 769–774.
[23] J. Zhao, T.M. Fyles, T.D. James, Angew. Chem. Int. Ed. 43 (2004) 3461–3464.
[24] W. Yang, X. Gao, B. Wang, Med. Res. Rev. 23 (2003) 346–368.
[25] R. Badugu, J.R. Lakowicz, C.D. Geddes, Bioorg. Med. Chem. 13 (2005) 113–119.
[26] T. Kunitake, Y. Okahata, J. Am. Chem. Soc. 102 (1980) 549–553.
[27] X. Gao, Y. Zhang, B. Wang, Tetrahedron 61 (2005) 9111–9117.
[28] T.D. James, K.R.A. Samankumara, R. Iguchi, S. Shinkai, J. Am. Chem. Soc. 117 (1995) 8982–8987.
[29] S. Fery-Forgues, M.T. Le Bris, J.-P. Guette, B. Valeur, J. Phys. Chem. 92 (1988) 6233–6237.
[30] J. Fine, Br. Med. J. 1 (1965) 1209–1214.